Published in final edited form as:

Dev Dyn. 2018 June ; 247(6): 867–881. doi:10.1002/dvdy.24634.

Isolation of A Unique Hepatic Stellate Cell Population Expressing Integrin α8 from Embryonic Mouse Livers

Tomohiro Ogawa[1,2], **Yuchang Li**[1], **Ingrid Lua**[1], **Andrea Hartner**[3], and **Kinji Asahina**[1]

[1]Southern California Research Center for ALPD and Cirrhosis and Department of Pathology, Keck School of Medicine of the University of Southern California, Los Angeles, California

[2]Center for the Advancement of Higher Education, Faculty of Engineering, Kindai University, Hiroshima, Japan

[3]Department of Pediatrics and Adolescent Medicine, University Hospital of Erlangen, Erlangen, Germany

Abstract

Background—Hepatic stellate cells (HSCs) play an important role in liver fibrogenesis. However, little is known about their phenotype and role in liver development. The aim of this study is to identify specific markers for embryonic HSCs.

Results—Using antibodies against ALCAM and PDPN, we separated mesothelial cells (MCs) and HSCs from developing livers and identified integrin α8 (ITGA8) as a marker for embryonic desmin+ HSCs that are preferentially localized near the developing liver surface and α-smooth muscle actin+ perivascular mesenchymal cells around the vein. A cell lineage tracing study revealed that upon differentiation, MC-derived HSCs or perivascular mesenchymal cells express ITGA8 during liver development. Using anti-ITGA8 antibodies, we succeeded in isolating MC-derived HSCs and perivascular mesenchymal cells from embryonic livers. In direct coculture, ITGA8+ mesenchymal cells promoted the expression of hepatocyte and cholangiocyte markers in hepatoblasts. In the normal adult liver, expression of ITGA8 was restricted to portal fibroblasts in the portal triad. Upon liver injury, myofibroblasts increased the expression of ITGA8.

Conclusions—ITGA8 is a specific cell surface marker of MC-derived HSCs and perivascular mesenchymal cells in the developing liver. Our data suggest that ITGA8+ mesenchymal cells maintain the phenotype of hepatoblast in liver development.

Keywords

Alcam; mesothelial cells; Itga8; myofibroblasts; podoplanin; septum transversum mesenchyme

*Correspondence to: Kinji Asahina, Southern California Research Center for ALPD and Cirrhosis, Department of Pathology, Keck School of Medicine, University of Southern California, 1333 San Pablo Street, MMR 402, Los Angeles, CA 90033-9141, asahina@usc.edu.

GEO database for the microarray data: GSE107349 (reviewer token: unulqwuixdghlaj)

Introduction

Epithelial-mesenchymal interaction is essential in organ development and wound healing. In liver development, the definitive endoderm in the foregut begins to form the hepatic diverticulum around embryonic day (E) 8–9 in mice (Zaret, 2016). The endodermal cells invade into the surrounding septum transversum and differentiate into hepatoblasts in the developing liver. Hepatoblasts become mature hepatocytes and form the sinusoid structure with sinusoidal endothelial cells (Si-Tayeb et al., 2010). A subset of hepatoblasts adjacent to the portal area subsequently differentiates into biliary epithelial cells and forms the bile duct (Zong and Stanger, 2012). Hepatic stellate cells (HSCs) reside in the space of Disse between hepatocytes and sinusoidal endothelial cells and store vitamin A lipids in their cytoplasm in adult livers (Yin et al., 2013). Upon liver injury, HSCs lose vitamin A droplets, acquire myofibroblastic morphology, express extracellular matrix (ECM) proteins and inflammatory cytokines, and regulate the wound healing process (Tsuchida and Friedman, 2017). Quiescent HSCs express mesenchymal cell markers including desmin (DES) and vimentin (VIM) and increase the expression of type I collagen and α-smooth muscle actin (ACTA2) upon activation. Although HSCs also express neural cell markers including nestin and p75 neurotrophin receptor (NGFR), cell lineage tracing studies using *Mesp1*^{Cre} mice revealed that HSCs are mesodermal in origin (Asahina et al., 2009; Lua et al., 2014).

In the initial process of liver development, mesenchymal cells in the septum transversum interact with invading endodermal cells and form the hepatic diverticulum (Enzan et al., 1997). The septum transversum mesenchyme expresses Wilms tumor 1 homolog (WT1) and a cell lineage tracing study using *Wt1*^{CreERT2} mice showed that *Wt1*+ mesenchymal cells give rise to mesothelial cells (MCs) covering the liver surface and DES+ embryonic HSCs in developing livers (Asahina et al., 2011). MCs form a single epithelial layer of the mesothelium covering the internal organs and the wall of body cavities (Mutsaers, 2004). During liver development, *Wt1*+ MCs undergo mesothelial-mesenchymal transition, migrate inward from the liver surface, and give rise to DES+ HSCs in mice (Asahina et al., 2011). Interestingly, such conversion from MCs to HSCs also takes place in the adult livers upon injuries (Li et al., 2013). Similar to developing livers, mesothelial-mesenchymal transition has been reported in developing heart, lung, and intestine, and MCs are a unique source for mesenchymal cells in different organs (Armulik et al., 2011).

Cell surface markers are useful tools for characterization and isolation of target cells. Several studies reported identification of surface markers for liver MCs including CD200, glycoprotein M6A (GPM6A), mesothelin (MSLN), podoplanin (PDPN), and podocalyxin-like (PODXL) in embryonic and adult liver MCs (Asahina et al., 2009; Onitsuka et al., 2010; Li et al., 2013). Although NGFR was shown to be expressed in embryonic HSCs (Suzuki et al., 2008), antibodies capable of isolating these cells by fluorescence-activated cell sorting (FACS) are not readily available. In the present study, we separated MCs and MC-derived HSCs from developing liver by FACS and identified integrin α8 (ITGA8) as a cell surface marker for MC-derived HSCs and perivascular mesenchymal cells in mouse developing livers. We succeeded in isolating ITGA8+ mesenchymal cells from mouse embryonic livers using anti-ITGA8 antibodies.

Results

Identification of ITGA8 as A Novel Marker for MC-Derived HSCs in Developing Livers

In E12.5 mouse developing livers, MCs expressing PDPN are located on the basal lamina composed of type IV collagen on the liver surface (Fig. 1A). We previously reported that MCs migrate inward from the liver surface and give rise to HSCs (Asahina et al., 2011). Although several surface markers for MCs have been identified, few surface markers are available for isolation of fetal HSCs. To identify novel cell surface markers for embryonic HSCs, we attempted to separate MCs and HSCs from embryonic livers and determined gene expression by microarray. We previously reported that MCs and MC-derived HSCs near the developing liver surface express activated leukocyte cell adhesion molecule (ALCAM) (Fig. 1B–D) (Li et al., 2013). HSCs inside the liver express DES and NGFR and show no or weak expression of ALCAM compared to MC-derived HSCs near the liver surface (Fig. 1C,D). Given that both PDPN and ALCAM are cell surface markers, we attempted to separate MCs and MC-derived HSCs near the liver surface as ALCAM+ PDPN+ and ALCAM+ PDPN− cells, respectively. FACS analysis revealed the presence of ALCAM+ PDPN− (2.6%) and ALCAM+ PDPN+ (1.0%) populations in the E12.5 liver (Fig. 1E). Quantitative RT-PCR (QPCR) showed that ALCAM+ PDPN+ cells highly express MC markers, such as *Pdpn*, *Gpm6a*, and *Wt1* mRNAs (Fig. 1F). In contrast, the ALCAM+ PDPN− population expressed HSC markers, such as *Des* and *Ngfr* mRNAs (Fig. 1F), suggesting the enrichment of MC-derived HSCs. To identify cell surface markers for the ALCAM+ PDPN− MC-derived HSCs, we analyzed mRNA expression by microarray analysis. ALCAM+ PDPN+ MCs expressed MC markers, such as *Alcam*, *Pdpn*, *Gpm6a*, and *Wt1* genes (Table 1). We found that ALCAM+ PDPN− HSCs express *Itga8* (Table 2). QPCR confirmed the high expression of *Itga8* mRNA in ALCAM+ PDPN− HSCs compared to ALCAM+ PDPN+ MCs (Fig. 1F).

Expression of ITGA8 in Early Developing Livers

Although the expression of ITGA8 was previously reported in the mesenchymal cells of the developing kidney and lung (Muller et al., 1997), little was known about its expression in developing livers. We examined the expression of ITGA8 in mouse embryonic livers by immunofluorescence labeling. Mesenchymal cells in the septum transversum express ALCAM, DES, and ITGA8 (Fig. 2A,B). DES+ HSCs in E11.5 embryos express ITGA8 (Fig. 2C). ITGA8 is also expressed in ALCAM+ MC-derived HSCs near the liver surface and perivascular mesenchymal cells in the vascular wall (Fig. 2D). From E12.5 livers, the expression of ITGA8 becomes restricted to MC-derived HSCs expressing ALCAM, DES, and NGFR near the liver surface (Fig. 2E–G). ITGA8 is also expressed in the epicardium of the developing heart (Fig. 2E). The flat cell layer, which forms the diaphragm, between the developing liver and heart strongly express ALCAM and inner layers co-express ITGA8 (Fig. 2E). Perivascular mesenchymal cells expressing ACTA2 co-express ITGA8 in the vein (Fig. 2H). Chondroitin sulfate proteoglycan 4 (CSPG4/NG2), a marker for pericytes (Yamazaki et al., 2017), was weakly expressed in ITGA8+ perivascular mesenchymal cells (Fig. 2I). Its faint expression was also noted in HSCs and MCs in E12.5 embryonic livers (Fig. 2I). No ITGA8 expression is observed in PDPN+ MCs that are separated from ITGA8+ HSCs by type IV collagen (Fig. 2J,K). ITGA8+ HSCs are closely associated with FLK1+ CD31+ sinusoidal endothelial cells in the developing liver (Fig. 2L,M). E-cadherin

(CDH)1+ hepatoblasts, F4/80+ macrophages, and CD45+ leukocytes are negative for ITGA8 staining (Fig. 2N–P).

Expression of ITGA8 in Embryonic livers in Later Stages

From E15.5, the expression of ITGA8 is restricted in MC-derived HSCs that express DES and ALCAM beneath the liver surface (Fig. 3A–C). ITGA8+ MC-derived HSCs are located beneath PDPN+ MCs and type IV collagen in E16.5–17.5 livers (Fig. 3D–F). Perivascular mesenchymal cells remain positive for ITGA8 and CSPG4 in E17.5 livers (Fig. 3G). The expression of CSPG4 is weakly observed in MCs (Fig. 3H). Hepatoblasts around the portal vein initiate the expression of ALCAM from E17.5 (Fig. 3I). Immunofluorescence labeling of serial sections revealed the expression of ALCAM in cytokeratin 19 (KRT19)+ ductal plates formed near the portal vein (Fig. 3J).

MCs Give Rise to ITGA8+ HSCs during Liver Development

To determine whether MCs-derived HSCs initiate the expression of ITGA8 upon differentiation from MCs in developing liver, we injected tamoxifen to pregnant mice carrying E10.5 *Wt1*$^{\mathrm{CreERT2/+}}$; *Rosa26*mTmG$^{\mathrm{flox/+}}$ embryos. One day after tamoxifen injection, mesenchymal cells surrounding the liver bud expressed GFP+ (Fig. 4A). Three days after tamoxifen injection, GFP expression was observed in MCs and ALCAM+ cells near the liver surface (Fig. 4B). These GFP+ cells beneath the mesothelium co-express ITGA8 and DES (Fig. 4C,D), indicating the differentiation of MCs to ITGA8+ HSCs during liver development. We also observed the GFP expression in ITGA8+ perivascular mesenchymal cells in the vein (Fig. 4C). WT1 was expressed in MCs, but not in GFP+ HSCs in the developing liver (Fig. 4E). The cell lineage tracing indicates that, upon differentiation, MC-derived HSCs initiate the expression of ITGA8 and a subset of this population becomes perivascular mesenchymal cells on the wall of the vein during liver development.

Isolation of ITGA8+ Mesenchymal Cells from Embryonic Livers

Given that integrins are expressed on cell surface, we expected that MC-derived HSCs and perivascular mesenchymal cells could be isolated using anti-ITGA8 antibodies and FACS from embryonic livers. FACS analysis revealed the presence of ITGA8+ cells in E12.5 embryonic livers (Fig. 5A). QPCR confirmed that purified ITGA8+ cells express high *Itga8* mRNA and HSC genes including *Des* and *Ngfr* (Fig. 5B). We further separated E12.5 embryonic liver cells using antibodies for ITGA8 and ALCAM. FACS analysis showed the presence of these 2 populations in E12.5 livers (Fig. 5A). As expected, ALCAM+ ITAG8+ cells express HSC markers (Fig. 5B). In contrast, ALCAM+ ITGA8− cells express MC markers abundantly (Fig. 5B). Microarray analysis confirmed high expression of MC markers in ALCAM+ ITGA8− cells compared to ALCAM+ ITGA8+ cells (Table 1). The ALCAM+ ITGA8+ population showed high expression of *Itga8* mRNA and HSC markers such as *Lhx2* and *Ngfr* mRNAs (Table 1, 2). This population also expresses high *Acta2* mRNA expression (Table 1) in agreement with the expression of ITGA8 in ACTA2+ perivascular mesenchymal cells in the liver (Fig. 2H). Our data indicate that ITGA8 is a new cell surface marker for embryonic liver mesenchymal cells including HSCs and perivascular mesenchymal cells.

In Vitro Activation of Cultured ITGA8+ Mesenchymal Cells

To determine the role of ITGA8+ HSCs and perivascular mesenchymal cells in liver development, we isolated these mesenchymal cells from E12.5 livers using the anti-ITGA8 antibody and magnetic-activated cell sorting (MACS) and cultured on type I collagen (COL)-coated wells in DMEM containing 10% FBS. ITGA8+ mesenchymal cells exhibited fibroblastic morphology and expressed ITGA8, DES, and ACTA2 in culture (Fig. 6A,B). ITGA8 forms a heterodimer exclusively with integrin β1 and binds to several ECM proteins, such as fibronectin (FN) and nephronectin (NPNT), through the tripeptide sequence, RGD (Schnapp et al., 1995; Muller et al., 1997; Denda et al., 1998; Brandenberger et al., 2001). No morphological change was observed in ITGA8+ mesenchymal cells cultured on COL-, FN-, or NPNT-coated dishes (Fig. 6B). Among the ECM proteins tested, FN induced the growth of ITGA8+ mesenchymal cells compared to COL or NPNT (Fig. 6C). QPCR showed that ITGA8+ mesenchymal cells keep expressing *Itga8* mRNA on day 2 and 4 (Fig. 6D). Similar to *in vitro* activation of adult HSCs, ITGA8+ mesenchymal cells increased the expression of *Acta2* mRNA on day 7 (Fig. 6D), suggesting *in vitro* activation toward myofibroblasts. Cultured ITGA8+ mesenchymal cells expressed *Lhx2*, a transcription factor expressed in embryonic HSCs (Wandzioch et al., 2004), hepatocyte growth factor *(Hgf*), and pleiotrophin (*Ptn*) on day 2 and 4 cultured on different ECMs and their expression levels were increased on day 7 (Fig. 6D). To test the role of ITGA8 in embryonic ITGA8+ mesenchymal cells, we transfected with *Itga8* siRNAs. However, transfection with *Itga8* siRNAs did not change mRNA expression of *Acta2,* cyclin D1 (*Ccnd1*), *Hgf*, and *Ptn* in ITGA8+ cells cultured on different ECM-coated dishes (Fig. 6E,F).

ITGA8+ Mesenchymal Cells Maintain the Phenotype of Hepatoblasts in Coculture

Given that ITGA8+ mesenchymal cells express hepatotrophic factors including *Hgf* and *Ptn* genes, we expected that these cells promote the growth and function of hepatoblasts in developing liver. To test this assumption, we isolated hepatoblasts from E12.5 livers using anti-CDH1 antibodies and MACS. Hepatoblasts were cultured in serum free hepatoblast medium that was known to support their growth potential in culture. Before the coculture experiment, we tested whether embryonic ITGA8+ mesenchymal cells maintain their phenotype in the serum free hepatoblast medium. As shown in Fig. 7A, ITGA8+ mesenchymal cells grew well in this medium cultured on FN-coated wells (Fig. 7A). QPCR showed the induction of *Acta2* mRNA in ITGA8+ mesenchymal cells cultured on different ECMs (Fig. 7B). Cultured ITGA8+ mesenchymal cells keep expressing *Itga8*, *Lhx2*, *Hgf*, and *Ptn* mRNAs (Fig. 7B).

To test the effect of soluble factors secreted from ITGA8+ mesenchymal cells, we plated them in a cell culture insert coated with FN. After plating hepatoblasts in 24-wells, we transferred the cell culture insert to the hepatoblast wells and cocultured for 2 days in the hepatoblast medium. Two days after coculture, we measured DNA synthesis in hepatoblasts by the EdU incorporation assay. However, the EdU incorporation ratio was not changed in hepatoblasts cocultured with or without ITGA8+ mesenchymal cells (Fig. 7C,D). Hepatoblasts did not increase the expression of markers for hepatocytes (*Cdh1, Alb, Hnf4a, Cebpa, Cebpb, G6pc, and Cyp3a11*) in the presence of ITGA8+ mesenchymal cells (Fig. 7E). The expression of *Krt19* mRNA was decreased by coculture with ITGA8+

mesenchymal cells (Fig. 7E). These data suggest that soluble factors from ITGA8+ mesenchymal cells are not sufficient to promote the growth and function of hepatoblasts *in vitro*.

Next, we plated hepatoblasts in 24-wells, added ITGA8+ mesenchymal cells directly to the hepatoblast wells, and cocultured for 2 days. After EdU incorporation, hepatoblasts were stained with anti-CDH1 antibodies and the EdU+ hepatoblasts were counted (Fig. 7F). As shown in Fig. 7G, the EdU incorporation rate was not changed in hepatoblasts in the presence or absence of ITGA8+ mesenchymal cells. To analyze gene expression in cocultured hepatoblasts, we digested cocultured cells by Dispase and separated CDH1+ hepatoblasts by MACS. QPCR revealed that CDH1+ hepatoblasts significantly increase approximately two-fold the expression of *Cdh1, Alb, Krt19, Hnf4a*, and *Cebpb* mRNAs by coculturing with ITGA8+ mesenchymal cells (Fig. 7H). These data suggest that cell-cell contact and/or paracrine factors from ITGA8+ mesenchymal cells maintain the function of hepatoblasts.

Induction of ITGA8 Expression in Myofibroblasts in Biliary Fibrosis

The expression of ITGA8 was previously reported in myofibroblasts in adult rat fibrotic livers (Levine et al., 2000). Chronic liver injury induces accumulation of myofibroblasts that synthesize collagen and proinflammatory cytokines and promote fibrogenesis. The origin of myofibroblasts has been shown to be heterogeneous including HSCs, portal fibroblasts in the portal triad, and MCs (Wells and Schwabe, 2015). Since ITGA8 is uniquely expressed in MC-derived HSCs and perivascular mesenchymal cells in developing liver, we further examined its expression pattern in adult liver. Immunofluorescence labeling showed that expression of ITGA8 is weak in DES+ HSCs in the sinusoid of the normal adult mouse liver (Fig. 8A). In the portal triad, ITGA8 is expressed in portal fibroblasts that express DES and elastin (ELN) (Fig. 8A,B) (Lua et al., 2016). No ITGA8 expression was observed in GPM6A+ MCs (Fig. 8C). After surgical ligation of the extrahepatic bile duct, cholestasis causes damages around the portal vein in the liver, induces the myofibroblastic activation of both portal fibroblasts and HSCs, and results in biliary fibrosis. Two weeks after bile duct ligation in mice, myofibroblast around the bile duct co-expressed ITGA8, DES, ACTA2, and ELN (Fig. 8E–G). To analyze the expression of ITGA8 in activation of HSCs, we induced liver fibrosis by injection of CCl_4 that causes damage to hepatocytes around the central vein and induces fibrosis. After CCl_4 injection, HSCs are activated and express ACTA2 near damaged hepatocytes around the central vein (Fig. 8H). These ACTA2+ activated HSCs co-expressed ITGA8 (Fig. 8H). In the CCl_4-induced liver fibrosis model, MCs are known to differentiate into ACTA2+ myofibroblasts beneath the mesothelium (Li et al., 2013). Immunofluorescence labeling showed that myofibroblasts beneath GPM6A+ MCs co-express ITGA8 (Fig. 8I,J). These data indicate that ITGA8 is a maker for myofibroblasts in liver fibrosis.

Discussion

Upon liver injury, HSCs become myofibroblasts and participate in fibrogenesis. Although the molecular and cellular mechanisms underlying the activation of HSCs to myofibroblasts

have been extensively studied in liver fibrosis, little is known about their phenotype and role in liver development because isolation methods of embryonic HSCs are limited. In the present study, we identified ITGA8 as a cell surface marker for embryonic HSCs and perivascular mesenchymal cells. We previously identified PDPN as a cell surface marker for MCs and ALCAM in both MCs and HSCs near the liver surface in developing liver (Asahina et al., 2009). Our strategy in the present study was that HSCs would be isolated as ALCAM+ PDPN− cells from embryonic livers and genes expressed in these cells would be highlighted by the comparison of their gene expression profile with that of ALCAM+ PDPN + MCs. In fact, microarray analysis revealed that ALCAM+ PDPN− population highly expresses ITGA8. Isolated ITGA8+ mesenchymal cells express HSC markers including *Des* and *Ngfr* mRNAs and show fibroblastic morphology. Our data indicate that anti-ITGA8 antibodies are useful for isolation of MC-derived HSCs and perivascular mesenchymal cells from developing livers by FACS or MACS.

During liver development, *Wt1*+ mesenchymal cells in the septum transversum give rise to embryonic MCs and HSCs (Asahina et al., 2011). *Wt1*+ MCs migrate inward from the liver surface and give rise to HSCs. In the present study, we detected the expression of ITGA8 in the septum transversum mesenchyme in E9.5 and embryonic HSCs from E11.5. Interestingly, the expression of ITGA8 is restricted in HSCs near the liver surface and perivascular mesenchymal cells around the vein from E12.5 livers. The cell lineage tracing of *Wt1*+ MCs revealed that upon differentiation from MCs, MC-derived HSCs lose the expression of MC markers and gain the expression of ITGA8. HSCs inside the liver are largely negative for ITGA8. Thus, ITGA8 is a unique marker for MC-derived HSCs near the liver surface and perivascular mesenchymal cells around the vein from E12.5 livers. We separated MCs and MC-derived HSCs as ALCAM+ ITGA8− and ALCAM+ ITGA8+ cells by FACS from E12.5 livers. Microarray analysis showed that ALCAM+ ITGA8+ cells express low levels of MC markers (*Cd200*, *Gpm6a*, *Krt19*, and *Upk1b*) compared to ALCAM+ ITGA8− and ALCAM+ PDPN+ MCs. However, ALCAM+ ITGA8+ cells express relatively high levels of *Pdpn* and *Wt1* mRNAs compared to ALCAM+ PDPN− cells. We previously reported that there are few MC-derived HSCs that weakly express WT1 in E12.5 livers (Asahina et al., 2011). Although immunofluorescence staining shows the high expression of PDPN in MCs, we cannot exclude the possibility that transient cells from MCs to HSCs may still express PDPN weakly and these cells are sorted into the ALCAM+ ITGA8+ population by FACS. Post-transcriptional control mechanisms of *Pdpn* gene may also be involved in its mRNA expression in ALCAM+ ITGA8+ cells. Microarray analysis showed ALCAM+ ITGA8+ population express *Tgfb1, Tgfb2*, and *Vegfc* mRNAs compared to other populations (Table 2). ITGA8+ perivascular mesenchymal cells might be the source of these factors in developing livers.

Microarray analysis revealed that embryonic liver ALCAM+ PDPN+ MCs and ALCAM+ PDPN− HSCs express PTN and midkine (MDK) (Table 2) that are known to induce the proliferation of hepatoblasts (Asahina et al., 2002; Onitsuka et al., 2010; Ito et al., 2014). Similar to MCs, embryonic HSCs express *Fgf11*, *Hgf*, and *Pdgfa* mRNAs. We expected that ITGA8+ mesenchymal cells induce the proliferation and differentiation of hepatoblasts during liver development. However, ITGA8+ mesenchymal cells did not induce DNA synthesis in hepatoblasts in indirect or direct coculture. Interestingly, ITGA8+ mesenchymal

cells induced the expression of several hepatocyte (*Cdh1, Alb, Hnf4a, Cebpb*) and cholangiocyte (*Krt19*) markers when both cells were cocultured directly. Our data suggest that cell-cell contacts and/or paracrine factors from ITGA8+ mesenchymal cells are necessary to maintain the phenotype of hepatoblasts. Further studies are necessary to determine whether hepatoblasts may control their phenotypes by modulating the phenotype of ITGA8+ mesenchymal cells. Interactions of embryonic HSCs with other cell types, including sinusoidal endothelial cells and blood cells, might be necessary to control the growth and differentiation of hepatoblasts.

Integrin is composed of non-covalently associated α and β subunits. There are 18 α and 8 β chains, which form at least 24 integrins (Barczyk et al., 2010). ITGA8 forms heterodimers exclusively with integrin β1 and binds to NPNT, FN, vitronectin, tenascin, and osteopontin (Schnapp et al., 1995; Denda et al., 1998; Linton et al., 2007). Among RGD-containing ECM proteins, integrin α8β1 preferentially binds to NPNT (Sato et al., 2009). *Itga8* knockout mice show severe defects in kidney development and interaction of integrin α8β1 and NPNT is essential for the invasion of the ureteric bud into the metanephric mesenchyme (Muller et al., 1997; Linton et al., 2007). In the present study, we found that isolated ITGA8+ mesenchymal cells grew well on FN-coated dishes compared to NPNT-coated dishes. Although ITGA8+ MC-derived HSCs are negative for ACTA2, a marker for myofibroblasts, in developing livers, they expressed ACTA2 on FN-coated dishes. On the other hand, ITGA8+ mesenchymal cells on NPNT-coated dishes express low levels of ACTA2, suggesting that the phenotype of HSCs is regulated by different ECM proteins in liver development. Knock down of *Itga8* using siRNAs did not show noticeable changes in cultured ITGA8+ mesenchymal cells. Although *Itga8* knockout mice show severe defects in kidney development, a few *Itga8*-knockout mice carry one kidney and the survivors grow normally (Muller et al., 1997). Although ITGA8 is strongly expressed in MC-derived HSCs in developing liver, no abnormalities were reported in *Itga8*-knockout embryonic livers. Integrin β1 forms heterodimer with different integrin α chains including α5 and αv and binds to RGD-containing extracellular matrix proteins. Microarray data showed that embryonic ITGA8+ HSCs express *Itgb1*, *Itga5*, and *Itgav* mRNAs (Table 2). Other integrin β1 partners might compensate the loss of ITGA8 in HSCs in liver development.

In adult tissues, expression of ITGA8 is restricted to vascular and visceral smooth muscle cells, mesangial cells in the kidney, and alveolar myofibroblasts (Levine et al., 2000; Hartner et al., 2009; Hartner et al., 2012). Up-regulation of ITGA8 is reported in organ fibrosis including the heart, lung, liver, and kidney (Levine et al., 2000; Bouzeghrane et al., 2004; Hartner et al., 2012). In the normal adult liver, the expression of ITGA8 is observed in portal fibroblasts around the portal vein and its expression is weak in HSCs. Upon liver injury caused by bile duct ligation, myofibroblasts around the portal vein express ITGA8, suggesting that ITGA8 is uniquely expressed in portal fibroblast-derived myofibroblasts in biliary fibrosis. In CCl_4-induced fibrosis, HSC-derived myofibroblasts strongly express ITGA8. In hepatitis, NPNT was shown to be involved in recruitment of inflammatory cells (Inagaki et al., 2013). It remains to be clarified how integrin α8β1-NPNT participates in liver injury and fibrogenesis.

In conclusion, we identified ITGA8 as a specific marker for MC-derived HSCs and perivascular mesenchymal cells in developing liver and myofibroblasts in adult liver fibrosis. ITGA8 is a useful marker for isolation of embryonic liver mesenchymal cells.

Experimental Procedures

Mice

Wt1^{CreERT2} mice were obtained from Dr. William Pu (Zhou et al., 2008). C57BL/6 and *Rosa26*mTmG^{flox} mice (Muzumdar et al., 2007) were purchased from Jackson Laboratory. Tamoxifen (Sigma-Aldrich, St. Louis, MO) dissolved in ethanol was emulsified in sesame oil (12.5 mg/ml) and was injected intraperitoneally to the pregnant mice carrying E10.5 embryos at 100 μg/g body weight. One or 3 days after tamoxifen injection, we collected embryos for immunofluorescence labeling.

To induce biliary fibrosis, mice were subjected to bile duct ligation for 2 weeks (Li et al., 2013). Fibrosis was induced by subcutaneous injection of CCl_4 (1 ml/kg body weight, 3 mice) with mineral oil in a 1:3 dilution every third day for a total of 9 injections. Mice were used in accordance with protocols approved by the IACUC of the University of Southern California.

Immunofluorescence Staining

Tissues were fixed with 4% paraformaldehyde in PBS for 4 hr and incubated with 15% sucrose in PBS for 4 hr at 4 °C. After incubating with 30% sucrose in PBS overnight, tissues were embedded in Tissue Freezing Medium (GeneralData, Cincinnati, OH). Sections were cut at 7 μm in a cryostat (CM1900; Leica, Buffalo Grove, IL). After washing with PBS, sections were partially digested with 20 μg/mL proteinase K (ThermoFisher Scientific, Waltham, MA) for 3 min and were blocked with 5% serum for 30 min. After blocking, the sections were incubated with the primary antibodies for ACTA2-FITC or Cy3 (C6198; Sigma-Aldrich, 200-fold dilution), ALCAM (14-1661; eBioscience, San Diego, CA, 100-fold dilution), CD45 (14-0451; 200-fold dilution), F4/80 (14-4801; 500-fold dilution), FLK1 (14-5821; 50-fold dilution), PDPN (14-5381; 100-fold dilution), CD31 (550274; BD Biosciences, San Jose, CA, 100-fold dilution), CDH1 (13-1900; Zymed, South San Francisco, CA, 1,000-fold dilution), type IV collagen (AB756P; Millipore, Temecula, CA, 200-fold dilution), DES (RB-9014; ThermoFisher Scientific, 300-fold dilution), GFP (A11122; 1,000-fold dilution), GFP (04404-84; Nacalai USA, San Diego, CA, 800-fold dilution), ELN (CL55041AP; Cedarlane, Burlington, NC, 200-fold dilution), GPM6A (D055-3; MBL, Woburn, MA, 500-fold dilution), NG2 (AB5320; Millipore, Temecula, CA, 50-fold dilution), NGFR (ab8874; Abcam, Cambridge, MA, 1,000-fold dilution), and WT1 (6F-H2; Cell Marque, Rocklin, CA, 50-fold dilution) for 1 hr at room temperature as previously described (Asahina et al., 2009; Li et al., 2013; Lua et al., 2014). ITGA8 was detected with goat anti-mouse ITGA8 antibodies (AF4076; R&D systems, Minneapolis, MN, 100-fold dilution). The primary antibodies were detected with secondary antibodies conjugated with Alexa Fluor 488 and 568 dyes (ThermoFisher Scientific) by incubation for 30 min. The sections were counterstained with DAPI and were observed under a fluorescence microscope (90i; Nikon, Melville, NY).

FACS

E12.5 livers were digested with 0.25% trypsin/EDTA at 37°C for 5 min. After washing cells with DMEM containing 10% FBS and 10 μg/ml DNaseI twice, blood cells were eliminated by autoMACS using lineage cell depletion kit (130-090-858; Miltenyi Biotech). Then, cells were incubated with PE-labeled rat anti-mouse ALCAM antibodies (12-1661, eBioscience), Alexa Fluor 488-labeled hamster anti-mouse PDPN antibodies (53-5381, eBioscience), and/or goat anti-mouse ITGA8 antibody (R&D systems) for 30 min. After washing the cells with PBS 3 times, cells were incubated with donkey anti-goat FITC secondary antibodies (F0109, R&D systems) for detection of the goat anti-ITGA8 antibody. The cells were analyzed using FACS Vantage SE (Becton Dickinson, San Jose, CA) as previously reported (Asahina et al., 2009).

QPCR

Total RNA was extracted with RNAqueous Micro and cDNA was synthesized using SuperScript III kit (ThermoFisher Scientific) as previously reported (Asahina et al., 2009). QPCR was performed with SYBR FAST qPCR kit (KAPA Biosystems, Wilmington, MA) in ViiA7 Real-Time PCR System (Applied Biosystems, Carlsbad, CA). Primer sequences are *Itga8* (5′-AGG CGA AAG TGC AGT CCT AA-3′ and 5′-GAA CCA GCA AAC CAA GAA GG-3′), *Hnf4a* (5′-TAC ATC AAC GAC CGG CAG TA-3′ and 5′-CCC ATG TGT TCT TGC ATC AG-3′), *Cebpa* (5′-AGC CGA GAT AAA GCC AAA CA-3′ and 5′-AAA CCA TCC TCT GGG TCT CC-3′), *Cebpb* (5′-AGA AGA CGG TGG ACA AGC TG-3′ and 5′-CAA GTT CCG CAG GGT GCT-3′), *G6pc* (5′-TCT TCA AGT GGA TTC TGT TTG G-3′ and 5′-GAC AGG GAA CTG CTT TAT TAT AGG-3′), and *Cyp3a11* (5′-CAC TTT CCT TCA CCC TGC AT-3′ and 5′-CTG TTG ACC CTT TGG GGA TA-3′). The primer sequences for *Acta2*, *Alb*, *Alcam*, *Ccnd1*, *Cd31*, *Cdh1*, *Des*, *Gapdh*, *Gpm6a*, *Hgf*, *Krt19*, *Lhx2*, *Ngfr*, *Pdpn*, *Ptn*, and *Wt1* were the same as described previously (Asahina et al., 2009; Li et al., 2013; Lua et al., 2014). The samples were run in triplicate. The relative mRNA levels per samples were calculated by subtracting the detection limit (40 Ct) from the cycle threshold value (Ct) of each gene in the same sample to obtain the ΔCt value. Taking the log2 of −ΔCt resulted in the relative expression value of each gene for each sample expressed in arbitrary units. Each value was normalized against to that of *Gapdh*.

Microarray Analysis

After FACS sorting, total RNA was extracted and the probes for the microarray were synthesized using the Ovation RNA amplification system V2 (NuGEN, San Carlos, CA) as previously described (Asahina et al., 2009). The labeled probes were hybridized with GeneChip Mouse Genome 430 2.0 arrays (Affymetrix, Santa Clara, CA) at the Molecular Pathology Genomics Core of the Children's Hospital Los Angeles and signals were analyzed with Genomic Suite Software (Partek, St. Louis, MO) at the USC Norris Medical Library. The microarray data were deposited in the GEO database (accession no. GSE107349).

Isolation and Culture of ITGA8+ Mesenchymal cells

E12.5 livers were digested with trypsin/EDTA as above and liver cells were suspended in DMEM containing 10% FBS. Cells were incubated with biotinylated goat anti-mouse ITGA8 antibody (BAF4076; R&D systems, 5 μg/ml) for 30 min. After washing, cells were incubated with anti-biotin microbeads (130-090-485; Miltenyi Biotec, San Diego, CA) and ITGA8+ cells were separated by autoMACS Pro Separator (Miltenyi Biotec) by the Integrative Liver Cell Core (R24AA012885). The yield of ITGA8+ cells was around 1–$2x10^5$ cells from one E12.5 liver. 24-well plates were coated with type I collagen (Advanced BioMatrix, San Diego, CA, 3 mg/ml), FN (Sigma-Aldrich, 10 μg/ml), or NPNT (R&D Systems, 10 μg/ml) for 2 hr. ITGA8+ cells ($1x10^5$ cells) were plated on the coated dishes and were cultured in DMEM containing 10% FBS or hepatoblast medium consisting of DMEM/F-12, B-27 supplement (ThermoFisher Scientific), ITS-X, 10 mM HEPES, and Penicillin-Streptomycin (Tsuchiya et al., 2005). On day 2, 4, and 7, cells were incubated with 0.6 ml of trypsin/EDTA and the cell numbers were counted using a hemocytometer.

To knock-down the ITGA8 expression, cells were transfected with scrambled or *Itga8* siRNAs (241226; Dharmacon, Chicago, IL, 60 pmol per well) using Lipofectamine 2000 (ThermoFisher Scientific) according to their protocol. Cells were analyzed by QPCR and immunocytochemistry 2 days after lipofection.

Cultured ITGA8+ cells were fixed with 4% paraformaldehyde in PBS for 15 min. After washing with PBS, cells were blocked with 5% donkey serum in PBS for 30 min and then incubated with the primary antibodies for goat-anti-mouse ITGA8 (R&D Systems, 100-fold dilution) and DES (ThermoFisher Scientific, 400-fold dilution) or ACTA2-Cy3 (Sigma-Aldrich, 400-fold dilution) for 1 hr. The primary antibodies were detected with secondary antibodies conjugated with Alexa Fluor 488 and 568 dyes. The images were captured with EVOS imaging system (ThermoFisher Scientific).

Coculture of Hepatoblasts and ITGA8+ Mesenchymal Cells

For hepatoblast isolation, E12.5 livers were digested in DMEM medium containing 25 mM HEPES and 100 mg/ml Dispase II (ThermoFisher Scientific) for 30 min as previously described (Nitou et al., 2002; Shikanai et al., 2009). After digestion, cells were incubated with rat-anti-mouse CDH1 antibodies (ECCD-1; Takara Bio, Mountain View, CA, 50-fold dilution) in the presence of 10 mM $CaCl_2$ for 30 min. After washing, cells were incubated with anti-rat IgG microbeads (Miltenyi Biotec) and CDH1+ hepatoblasts were separated by autoMACS Pro Separator. Hepatoblasts ($1x10^4$ cells) were plated on FN-coated 24-wells and were cultured in hepatoblast medium. For indirect coculture, ITGA8+ mesenchymal cells ($5x10^4$ cells) were plated into a transwell (0.4 μm pore, Corning, NY) coated with FN. Hepatoblasts actively grow in this culture condition compared to ITGA8+ mesenchymal cells. To examine the effect of ITGA8+ mesenchymal cells on hepatoblasts, we plated 5 times more mesenchymal cells in coculture. One day after plating, the transwells were transferred to the hepatoblast wells and were cocultured in the hepatoblast medium for 2 days. For direct coculture, $5x10^4$ ITGA8+ mesenchymal cells were added to hepatoblasts wells. Two days after coculture, hepatoblasts were incubated with EdU (5-ethynyl-2′-deoxyuridine, 5 μM) in the culture medium for 1 hr. After fixation with 4%

paraformaldehyde, the incorporated EdU was detected using Click-iT plus EdU AlexaFluor594 imaging kit (ThermoFisher Scientific). Then, hepatoblats were stained with goat anti-mouse ALB antibodies (A90-134A; Bethyl, Montgomery TX, 200-fold dilution) or mouse anti-CDH1 antibody conjugated with Alexa Fluor 488. The ALB antibody was detected with donkey anti-goat IgG conjugated with Alexa Fluor 488. The nuclei were counterstained with Hoechst 33342 and signals were detected with EVOS imaging system. Twenty images were randomly captured with a x20 objective. The experiment was repeated 3 times.

For measurement of gene expression in hepatoblasts cocultured with ITGA8+ mesenchymal cells, cocultured cells on day 2 were incubated with DMEM medium containing 25 mM HEPES and 100 mg/ml Dispase II (ThermoFisher Scientific) for 15 min and cells were incubated with rat-anti-mouse CDH1 antibodies (ECCD-1; Takara Bio, 50-fold dilution). After washing, cells were incubated with anti-rat IgG microbeads (Miltenyi Biotec) and CDH1+ hepatoblasts were separated by autoMACS Pro Separator for QPCR.

Statistical Analysis

Statistical tests for the significance of differences were assessed by using a Student's t-test or one-way ANOVA followed by a Tukey HSD post-hoc test. A P value of less than 0.05 was considered statistically significant.

Acknowledgments

Grant sponsor: NIH; Grant numbers: R01AA020753, pilot project funding from P50AA011999, R21AA024840.

We thank Ms. Meng Li for analysis of microarray data and Drs. Bin Zhou and William Pu for providing *Wt1*^{CreERT2} mice.

References

Armulik A, Genove G, Betsholtz C. Pericytes: developmental, physiological, and pathological perspectives, problems, and promises. Dev Cell. 2011; 21:193–215. [PubMed: 21839917]

Asahina K, Sato H, Yamasaki C, Kataoka M, Shiokawa M, Katayama S, Tateno C, Yoshizato K. Pleiotrophin/heparin-binding growth-associated molecule as a mitogen of rat hepatocytes and its role in regeneration and development of liver. Am J Pathol. 2002; 160:2191–2205. [PubMed: 12057922]

Asahina K, Tsai SY, Li P, Ishii M, Maxson RE Jr, Sucov HM, Tsukamoto H. Mesenchymal origin of hepatic stellate cells, submesothelial cells, and perivascular mesenchymal cells during mouse liver development. Hepatology. 2009; 49:998–1011. [PubMed: 19085956]

Asahina K, Zhou B, Pu WT, Tsukamoto H. Septum transversum-derived mesothelium gives rise to hepatic stellate cells and perivascular mesenchymal cells in developing mouse liver. Hepatology. 2011; 53:983–995. [PubMed: 21294146]

Barczyk M, Carracedo S, Gullberg D. Integrins. Cell Tissue Res. 2010; 339:269–280. [PubMed: 19693543]

Bouzeghrane F, Mercure C, Reudelhuber TL, Thibault G. Alpha8beta1 integrin is upregulated in myofibroblasts of fibrotic and scarring myocardium. J Mol Cell Cardiol. 2004; 36:343–353. [PubMed: 15010273]

Brandenberger R, Schmidt A, Linton J, Wang D, Backus C, Denda S, Muller U, Reichardt LF. Identification and characterization of a novel extracellular matrix protein nephronectin that is associated with integrin alpha8beta1 in the embryonic kidney. J Cell Biol. 2001; 154:447–458. [PubMed: 11470831]

Denda S, Reichardt LF, Muller U. Identification of osteopontin as a novel ligand for the integrin alpha8 beta1 and potential roles for this integrin-ligand interaction in kidney morphogenesis. Mol Biol Cell. 1998; 9:1425–1435. [PubMed: 9614184]

Enzan H, Himeno H, Hiroi M, Kiyoku H, Saibara T, Onishi S. Development of hepatic sinusoidal structure with special reference to the Ito cells. Microsc Res Tech. 1997; 39:336–349. [PubMed: 9407544]

Hartner A, Cordasic N, Rascher W, Hilgers KF. Deletion of the alpha8 integrin gene does not protect mice from myocardial fibrosis in DOCA hypertension. Am J Hypertens. 2009; 22:92–99. [PubMed: 19008864]

Hartner A, Menendez-Castro C, Cordasic N, Marek I, Volkert G, Klanke B, Rascher W, Hilgers KF. Tubulointerstitial de novo expression of the alpha8 integrin chain in a rodent model of renal fibrosis-a potential target for anti-fibrotic therapy? PLoS One. 2012; 7:e48362. [PubMed: 23144868]

Inagaki FF, Tanaka M, Inagaki NF, Yagai T, Sato Y, Sekiguchi K, Oyaizu N, Kokudo N, Miyajima A. Nephronectin is upregulated in acute and chronic hepatitis and aggravates liver injury by recruiting CD4 positive cells. Biochem Biophys Res Commun. 2013; 430:751–756. [PubMed: 23206711]

Ito K, Yanagida A, Okada K, Yamazaki Y, Nakauchi H, Kamiya A. Mesenchymal progenitor cells in mouse foetal liver regulate differentiation and proliferation of hepatoblasts. Liver Int. 2014; 34:1378–1390. [PubMed: 24238062]

Levine D, Rockey DC, Milner TA, Breuss JM, Fallon JT, Schnapp LM. Expression of the integrin alpha8beta1 during pulmonary and hepatic fibrosis. Am J Pathol. 2000; 156:1927–1935. [PubMed: 10854216]

Li Y, Wang J, Asahina K. Mesothelial cells give rise to hepatic stellate cells and myofibroblasts via mesothelial-mesenchymal transition in liver injury. Proc Natl Acad Sci U S A. 2013; 110:2324–2329. [PubMed: 23345421]

Linton JM, Martin GR, Reichardt LF. The ECM protein nephronectin promotes kidney development via integrin alpha8beta1-mediated stimulation of Gdnf expression. Development. 2007; 134:2501–2509. [PubMed: 17537792]

Lua I, James D, Wang J, Wang KS, Asahina K. Mesodermal mesenchymal cells give rise to myofibroblasts, but not epithelial cells, in mouse liver injury. Hepatology. 2014; 60:311–322. [PubMed: 24488807]

Lua I, Li Y, Zagory JA, Wang KS, French SW, Sevigny J, Asahina K. Characterization of hepatic stellate cells, portal fibroblasts, and mesothelial cells in normal and fibrotic livers. J Hepatol. 2016; 64:1137–1146. [PubMed: 26806818]

Muller U, Wang D, Denda S, Meneses JJ, Pedersen RA, Reichardt LF. Integrin alpha8beta1 is critically important for epithelial-mesenchymal interactions during kidney morphogenesis. Cell. 1997; 88:603–613. [PubMed: 9054500]

Mutsaers SE. The mesothelial cell. Int J Biochem Cell Biol. 2004; 36:9–16. [PubMed: 14592528]

Muzumdar MD, Tasic B, Miyamichi K, Li L, Luo L. A global double-fluorescent Cre reporter mouse. Genesis. 2007; 45:593–605. [PubMed: 17868096]

Nitou M, Sugiyama Y, Ishikawa K, Shiojiri N. Purification of fetal mouse hepatoblasts by magnetic beads coated with monoclonal anti-E-cadherin antibodies and their in vitro culture. Exp Cell Res. 2002; 279:330–343. [PubMed: 12243758]

Onitsuka I, Tanaka M, Miyajima A. Characterization and functional analyses of hepatic mesothelial cells in mouse liver development. Gastroenterology. 2010; 138:1525–1535. [PubMed: 20080099]

Sato Y, Uemura T, Morimitsu K, Sato-Nishiuchi R, Manabe R, Takagi J, Yamada M, Sekiguchi K. Molecular basis of the recognition of nephronectin by integrin alpha8beta1. J Biol Chem. 2009; 284:14524–14536. [PubMed: 19342381]

Schnapp LM, Hatch N, Ramos DM, Klimanskaya IV, Sheppard D, Pytela R. The human integrin alpha 8 beta 1 functions as a receptor for tenascin, fibronectin, and vitronectin. J Biol Chem. 1995; 270:23196–23202. [PubMed: 7559467]

Shikanai M, Asahina K, Iseki S, Teramoto K, Nishida T, Shimizu-Saito K, Ota M, Eto K, Teraoka H. A novel method of mouse ex utero transplantation of hepatic progenitor cells into the fetal liver. Biochem Biophys Res Commun. 2009; 381:276–282. [PubMed: 19217885]

Si-Tayeb K, Lemaigre FP, Duncan SA. Organogenesis and development of the liver. Dev Cell. 2010; 18:175–189. [PubMed: 20159590]

Suzuki K, Tanaka M, Watanabe N, Saito S, Nonaka H, Miyajima A. p75 Neurotrophin receptor is a marker for precursors of stellate cells and portal fibroblasts in mouse fetal liver. Gastroenterology. 2008; 135:270–281. [PubMed: 18515089]

Tsuchida T, Friedman SL. Mechanisms of hepatic stellate cell activation. Nat Rev Gastroenterol Hepatol. 2017

Tsuchiya A, Heike T, Fujino H, Shiota M, Umeda K, Yoshimoto M, Matsuda Y, Ichida T, Aoyagi Y, Nakahata T. Long-term extensive expansion of mouse hepatic stem/progenitor cells in a novel serum-free culture system. Gastroenterology. 2005; 128:2089–2104. [PubMed: 15940640]

Wandzioch E, Kolterud A, Jacobsson M, Friedman SL, Carlsson L. Lhx2−/ − mice develop liver fibrosis. Proc Natl Acad Sci U S A. 2004; 101:16549–16554. [PubMed: 15536133]

Wells RG, Schwabe RF. Origin and function of myofibroblasts in the liver. Semin Liver Dis. 2015; 35:97–106. [PubMed: 25974896]

Yamazaki T, Nalbandian A, Uchida Y, Li W, Arnold TD, Kubota Y, Yamamoto S, Ema M, Mukouyama YS. Tissue Myeloid Progenitors Differentiate into Pericytes through TGF-beta Signaling in Developing Skin Vasculature. Cell Rep. 2017; 18:2991–3004. [PubMed: 28329690]

Yin C, Evason KJ, Asahina K, Stainier DY. Hepatic stellate cells in liver development, regeneration, and cancer. J Clin Invest. 2013; 123:1902–1910. [PubMed: 23635788]

Zaret KS. From endoderm to liver bud: Paradigms of cell type specification and tissue morphogenesis. Curr Top Dev Biol. 2016; 117:647–669. [PubMed: 26970006]

Zhou B, Ma Q, Rajagopal S, Wu SM, Domian I, Rivera-Feliciano J, Jiang D, von Gise A, Ikeda S, Chien KR, Pu WT. Epicardial progenitors contribute to the cardiomyocyte lineage in the developing heart. Nature. 2008; 454:109–113. [PubMed: 18568026]

Zong Y, Stanger BZ. Molecular mechanisms of liver and bile duct development. Wiley Interdiscip Rev Dev Biol. 2012; 1:643–655. [PubMed: 23799566]

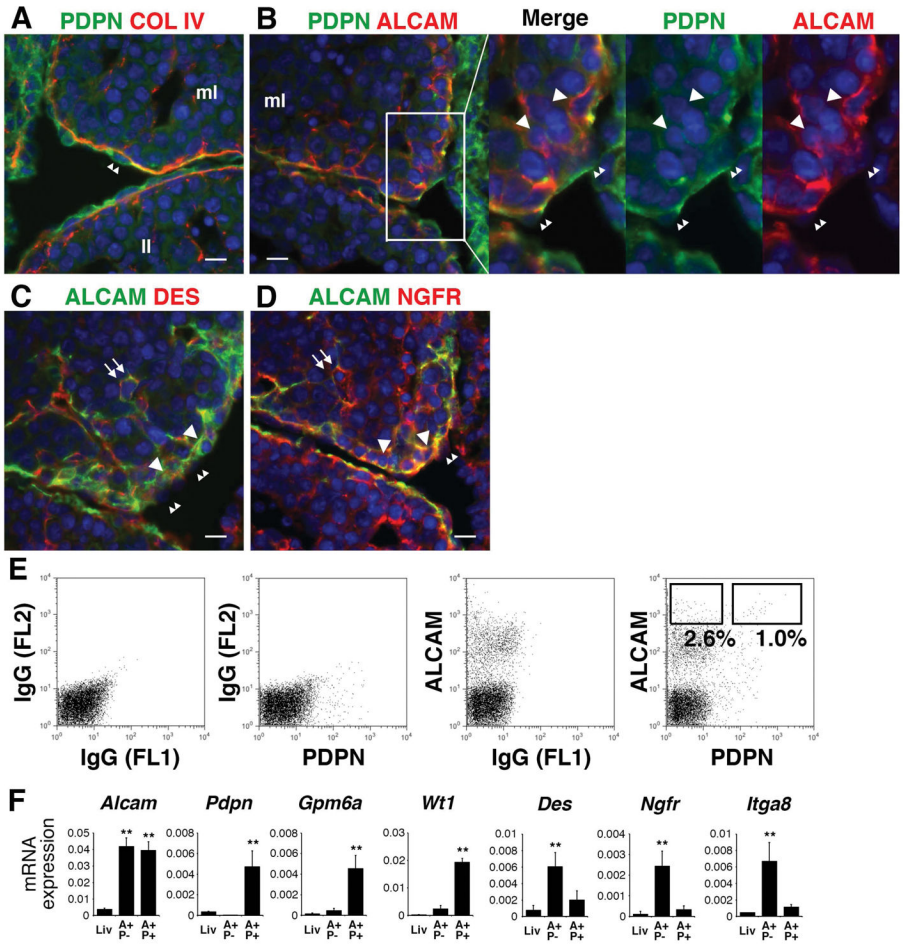

Figure 1.

Separation of MCs and MC-derived HSCs by FACS from E12.5 mouse embryonic livers. (A–D) Immunofluorescence labeling of PDPN, type IV collagen (COL IV), ALCAM, DES, and NGFR in E12.5 livers. Double arrowheads indicate MCs that express PDPN and ALCAM. Arrowheads indicate MC-derived HSCs that express ALCAM, DES, and NGFR beneath the mesothelium. Double arrows indicate DES+ NGFR+ HSCs that show weak ALCAM expression inside the liver. ll; left lobe, ml; median lobe. Nuclei were counterstained with DAPI. Bar, 10 μm. (E) FACS of E12.5 mouse livers. Liver cells were separated into ALCAM+ PDPN− and ALCAM+ PDPN+ populations by FACS. Control isotype IgGs were used as negative controls. (F) QPCR of the isolated ALCAM+ PDPN− (A+P−) and ALCAM+ PDPN+ (A+P+) populations in A. E12.5 liver cells before FACS were used as controls (Liv). The values were normalized against the *Gapdh* values. ** $P < 0.01$.

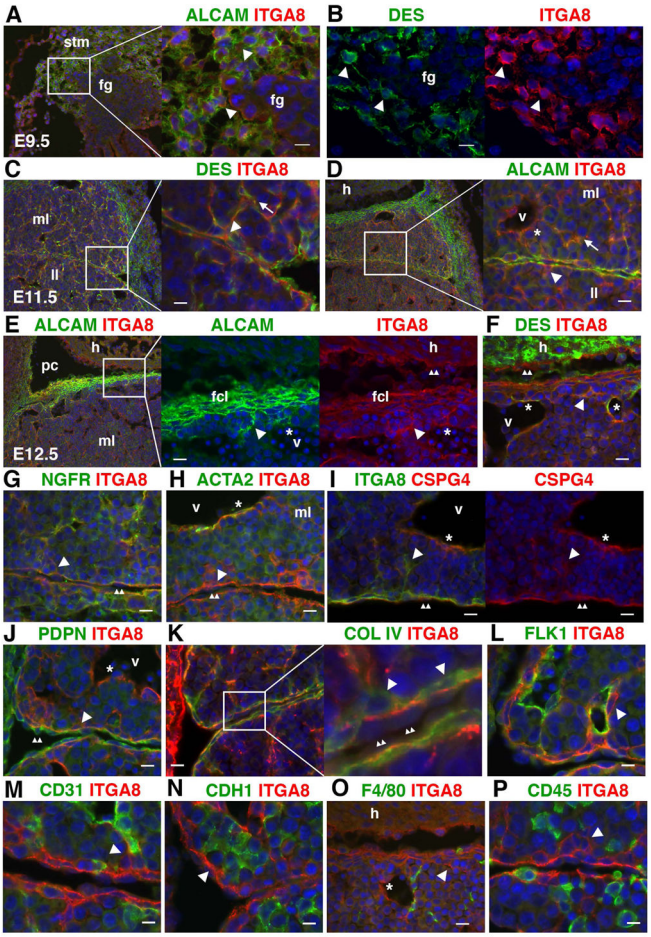

Figure 2.

Expression of ITGA8 in a subset of HSCs and perivascular mesenchymal cells in developing mouse livers. Immunofluorescence labeling of ITGA8 with different markers in E9.5 (A,B), E11.5 (C,D), and E12.5 (E–P) livers. (A,B) Mesenchymal cells in the septum transversum express ITGA8, ALCAM, and DES (arrowheads). fg; foregut, stm; septum transversum mesenchyme. (C,D) MC-derived HSCs (arrowheads), HSCs inside the liver (arrows), and perivascular mesenchymal cells (asterisks) around the vein express ITGA8, DES, and ALCAM in E11.5 livers. h; heart, ll; left lobe, ml; median lobe, v; vasculature. (E–G) Expression of ITGA8 becomes restricted in MC-derived HSCs (arrowheads) that express ALCAM, DES, and NGFR beneath the mesothelium. Double arrowheads indicate the epicardium (E,F) and MCs (G). fcl; flat cell layer, pc; pericardial cavity. (H) MC-derived HSCs (arrowhead) beneath the mesothelium (double arrowheads) and ACTA2+ perivascular mesenchymal cells (asterisks) express ITGA8. (I) CSPG4 is expressed in ITGA8+ perivascular mesenchymal cells (asterisks). Its weak expression is observed in MCs (double arrowheads) and HSCs (arrowheads). (J) Expression of ITGA8 in MC-derived HSCs underlying PDPN+ MCs. (K) ITGA8+ HSCs are separated from MCs by type IV collagen. (L–P) No expression of ITGA8 in FLK1+ CD31+ sinusoidal endothelial cells, CDH1+ hepatoblasts, F4/80+ macrophages, and CD45+ leukocytes.

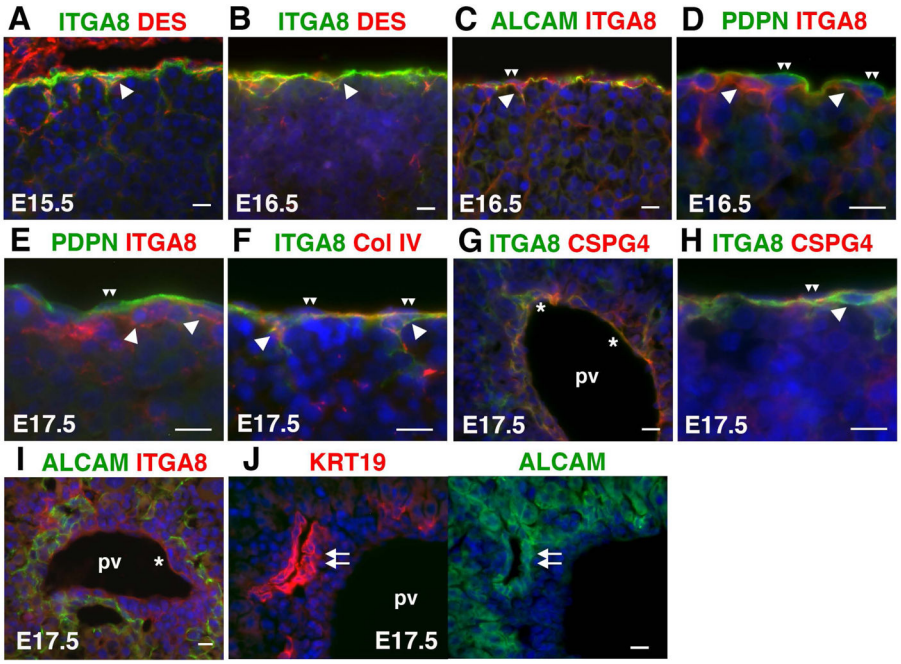

Figure 3.

Expression of ITGA8 in MC-derived HSCs and perivascular mesenchymal cells in developing livers in later stages. Immunofluorescence labeling of ITGA8 with different markers in E15.5 (A), E16.5 (B–D), and E17.5 (E–J) livers. (A–C) The expression of ITGA8 is restricted in MC-derived HSCs (arrowheads), which coexpress DES and ALCAM, near the liver surface at E15.5 and E16.5. (D–F) MC-derived HSCs expressing ITGA8 (arrowheads) are located beneath PDPN+ MCs (double arrowheads) and these two cell types are separated by COL IV. (G) Perivascular mesenchymal cells (asterisks) around the portal vein (pv) express ITGA8 and CSPG4. (H) MCs weakly express CSPG4. (I) Hepatoblasts around the portal vein also express ALCAM from this stage. (J) KRT19+ ductal plates (double arrows) formed near the portal vein express ALCAM. Nuclei were counterstained with DAPI. Bar, 10 μm.

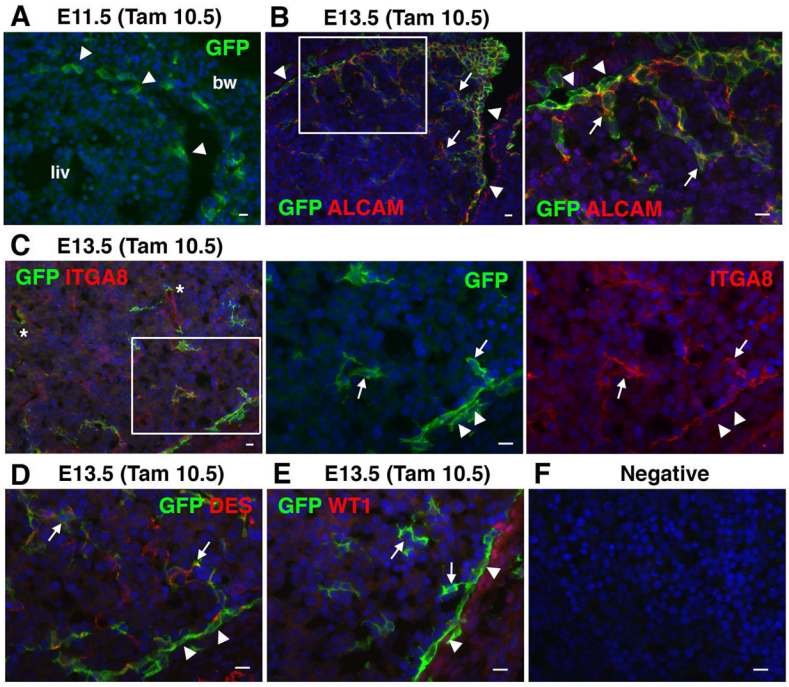

Figure 4.

MCs give rise to ITGA8+ HSCs during liver development. MCs were labeled with tamoxifen as GFP+ cells in E10.5 *Wt1*$^{CreERT2/+}$; *Rosa26*mTmG$^{flox/+}$ mouse embryos. (A) One day after tamoxifen injection, E11.5 livers were analyzed by immunofluorescence labeling of GFP. Arrowheads indicate GFP+ mesenchymal cells surrounding the developing liver (liv). bw, body wall. (B–E) E13.5 livers were analyzed by immunofluorescence labeling of GFP and ALCAM (B), ITGA8 (C), DES (D), or WT1 (E). Arrows indicate GFP + MC-derived HSCs that express ALCAM, ITGA8, and DES, but not WT1. MCs also give rise to GFP+ ITGA8+ perivascular mesenchymal cells (asterisks). Arrowheads indicate GFP + MCs. (F) GFP immunostaining in the control E13.5 *Wt1*$^{+/+}$; *Rosa26*mTmG$^{flox/+}$ embryo. No GFP expression is observed. The nuclei were counterstained with DAPI. Bar, 10 μm.

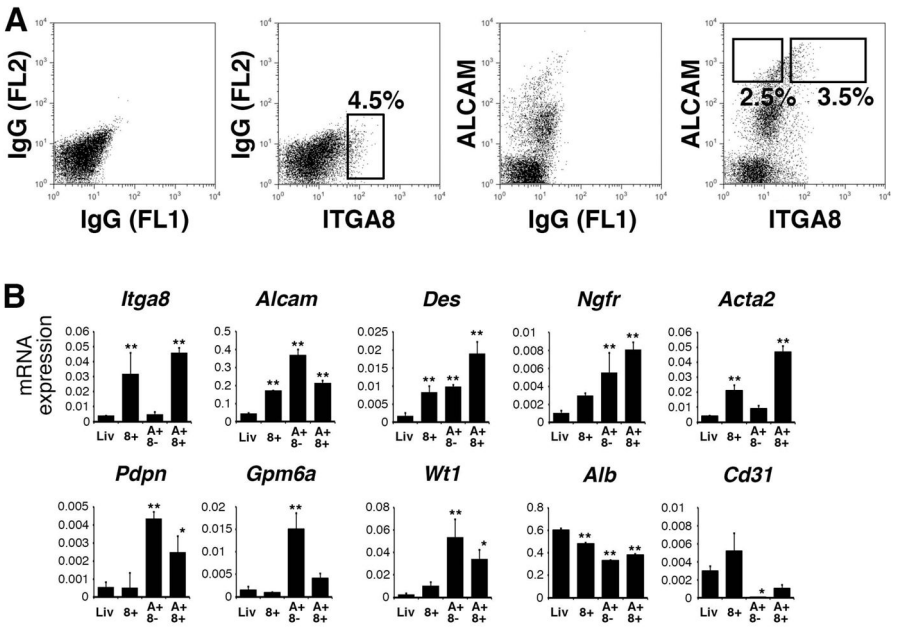

Figure 5.

Separation of ITGA8+ mesenchymal cells by FACS from E12.5 mouse embryonic livers. (A) FACS of E12.5 mouse livers shows the presence of ITGA8+ HSCs (4.5%). ITGA8+ cells were further separated into ALCAM+ ITGA8− and ALCAM+ ITGA8+ populations by FACS. Control isotype IgGs were used as negative controls. (B) QPCR of the isolated ITGA8+ (8+), ALCAM+ ITGA8− (A+8−) and ALCAM+ ITGA8+ (A+8+) populations in A. E12.5 liver cells before FACS were used as controls (Liv). The values were normalized against the *Gapdh* values. * $P < 0.05$, ** $P < 0.01$.

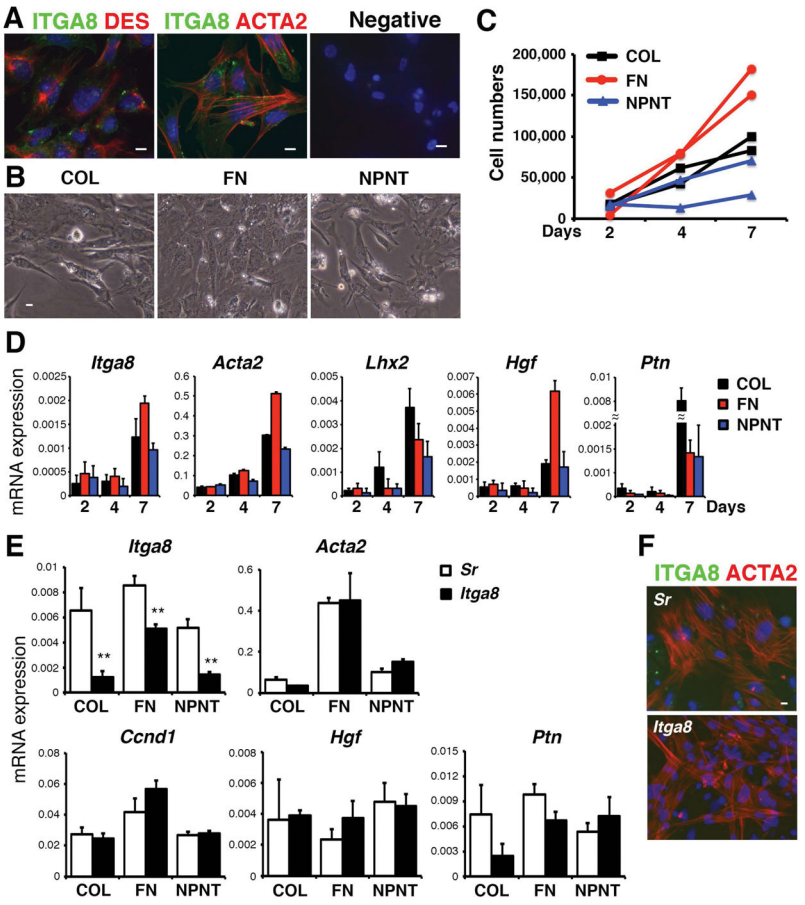

Figure 6.

Isolation of ITGA8+ mesenchymal cells from E12.5 mouse livers. (A) Immunofluorescence staining of ITGA8+ mesenchymal cells cultured on type I collagen (COL)-coated dishes for 1 day. Cultured mesenchymal cells express ITGA8 (green) and DES (red) or ACTA2. Cells stained without primary antibodies were used as a negative control. Nuclei were counterstained with DAPI. (B) Morphology of ITGA8+ mesenchymal cells cultured on COL-, FN-, or NPNT-coated dishes for 2 days. A representative experiment that was repeated two times is shown. (C) Growth of ITGA8+ mesenchymal cells on different ECM proteins in DMEM containing 10% FBS. (D) QPCR of cultured ITGA8+ mesenchymal cells on different ECM proteins. ITGA8+ mesenchymal cells increase the expression of *Itga8, Acta2, Lhx2, Hgf*, and *Ptn* mRNAs on day 7. The values were normalized against the *Gapdh* values. (E) Knock-down of *Itga8* gene with siRNAs in ITGA8+ mesenchymal cells cultured on different ECM proteins. Two days after treatment with siRNAs, expression of *Itga8*, *Acta2*, *Ccnd1*, *Hgf*, and *Ptn* mRNAs was analyzed by QPCR. siRNAs with scrambled sequence (Sr) were used as controls. ** $P < 0.01$. (F) Representative images of immunocytochemistry of ITGA8 (green) and ACTA2 (red) in ITGA8+ mesenchymal cells cultured on FN-coated dishes treated with *Sr* or *Itga8* siRNAs for 2 days. *Itga8* siRNAs reduce the expression of ITGA8 in cultured mesenchymal cells.

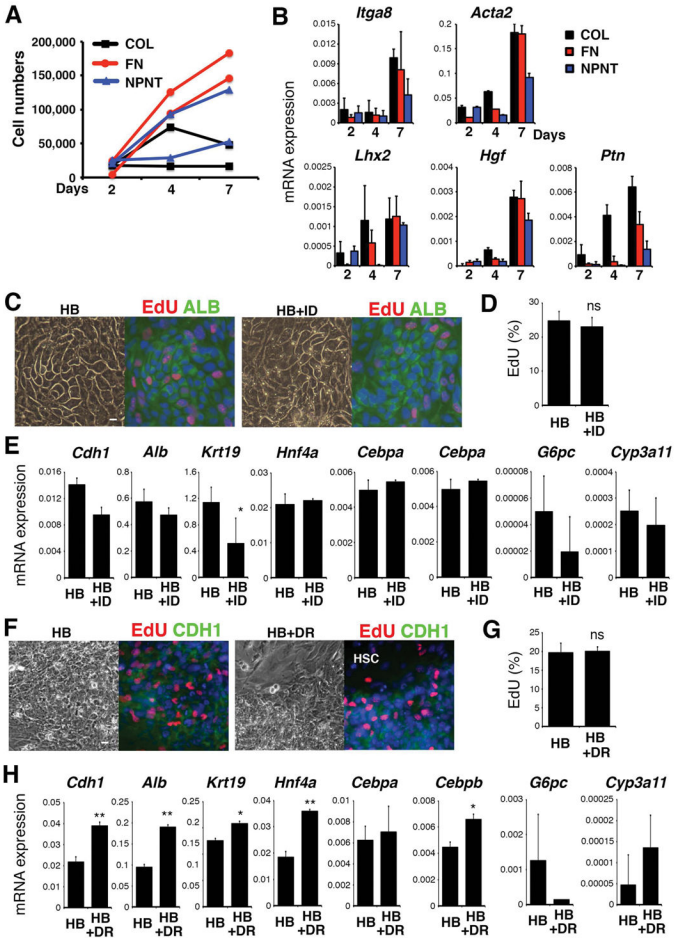

Figure 7.

Indirect and direct coculture of hepatoblasts with ITGA8+ mesenchymal cells. (A) Growth of ITGA8+ mesenchymal cells on different ECM proteins in serum free hepatoblast medium. (B) QPCR of cultured ITGA8+ mesenchymal cells on different ECM proteins. ITGA8+ mesenchymal cells increase the expression of *Itga8, Acta2, Lhx2, Hgf*, and *Ptn* mRNAs on day 7. The values were normalized against the *Gapdh* values. (C) Indirect coculture of hepatoblasts (HB) with or without ITGA8+ mesenchymal cells using a cell culture insert (+ID). Two days after coculture, the activity of DNA synthesis was assessed by EdU incorporation (red) in hepatoblasts. Hepatoblasts were stained with ALB (green) and the nuclei were counterstained with Hoechst 33342. A representative experiment that was repeated three times is shown. (D) Quantification of the EdU incorporation in hepatoblasts in C. Coculture with ITGA8A+ mesenchymal cells does not induce the DNA synthesis of hepatoblasts (7,207 and 7,164 hepatoblasts with or without coculture were counted, respectively). ns, statistically not significant. (E) QPCR of hepatoblasts in C. Indirect coculture of ITGA8+ mesenchymal cells does not induce the expression of hepatocyte and cholangiocyte markers in hepatoblasts. * $P < 0.05$. (F) Direct coculture of hepatoblasts (HB) with or without ITGA8+ mesenchymal cells (+DR). Two days after coculture, the activity of DNA synthesis was assessed by EdU incorporation (red) in hepatoblasts stained with CDH1 (green). A representative experiment that was repeated three times is shown. (G)

Quantification of the EdU incorporation in hepatoblasts in F. Coculture with ITGA8A+ mesenchymal cells does not induce the DNA synthesis of hepatoblasts (4,107 and 4,102 hepatoblasts with or without coculture were counted, respectively). (H) After coculture in F, cells were digested with Dispase and hepatoblasts were separated using anti-CDH1 antibodies by MACS. Separated CDH1+ hepatoblasts were subjected to QPCR. Direct coculture of ITGA8+ mesenchymal cells induces the expression of hepatocyte (*Cdh1, Alb, Hnf4a, Cebpb*) and cholangiocyte (*Krt19*) markers in hepatoblasts. No induction of mature hepatocyte markers (*G6pc* and *Cyp3a11*) was observed in hepatoblasts by direct coculture. ** $P < 0.01$. Bar, 10 μm.

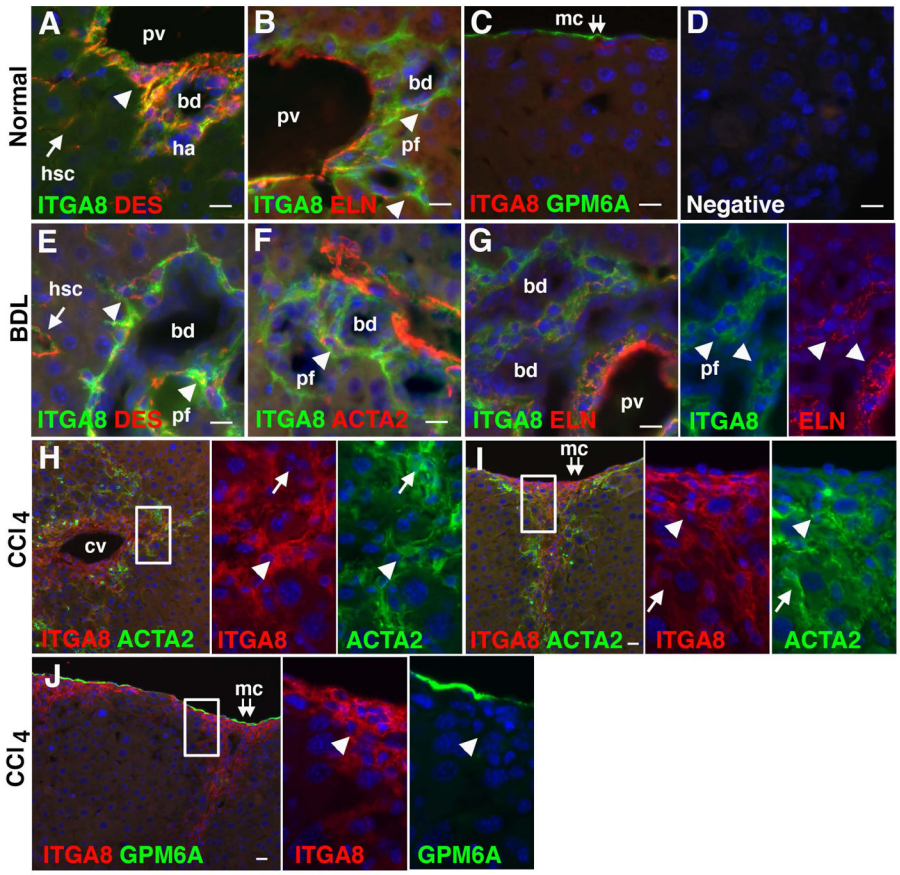

Figure 8.

Expression of ITGA8 in myofibroblasts in liver fibrosis. Immunofluorescence labeling of ITGA8 and DES, ELN, GPM6A, ACTA2, or ELN in the normal adult liver (A–D), biliary fibrosis induced by BDL (E–G), and liver fibrosis induced by CCl_4 (H–J). (A,B) Expression of ITGA8 is observed in portal fibroblasts (arrowheads) in the portal triad near the bile duct (bd) and portal vein (pv) in normal adult livers. Expression of ITGA8 is weak in DES+ HSCs (arrow). (C) No ITGA8 expression in GPM6A+ MCs (double arrows). (D) Negative control staining without primary antibodies. (E–G) Two weeks after BDL, portal fibroblasts express ITGA8, DES, ACTA2, and ELN (arrowheads). An arrow indicates HSCs that co-express ITGA8 and DES in biliary fibrosis. (H–J) In liver fibrosis induced by CCl_4 injections, ACTAT2+ myofibroblasts developed beneath GPM6A+ MCs (double arrows) express ITGA8 (arrowheads). An arrow indicates activated HSCs expressing ACTA2 and ITGA8. Nuclei were counterstained with DAPI. Bar, 10 μm.

Table 1

Microarray analysis: Expression of MC and mesenchymal cell markers.

Symbol	Liver	ALCAM+	ALCAM+ PDPN+ MCs	ALCAM+ PDPN− cells	ALCAM+ ITGA8− MCs	ALCAM+ ITGA8+ cells
MC markers						
Alcam	3,207	13,425	19,332	16,996	17,313	22,418
Cd200	25	379	1,874	56	683	261
Gpm6a	116	1,171	7,351	165	2,366	415
Krt19	59	871	5,676	164	4,781	756
Msln	8	62	430	22	153	48
Pdpn	100	3,877	7,746	117	6,176	4,658
Podxl	1,628	5,238	14,427	261	13,258	5,650
Upk1b	23	565	2,891	17	1,609	631
Wt1	102	1,994	7,554	691	6,421	5,762
Mesenchymal cell markers						
Acta2	302	1,939	2,092	2,005	1,808	4,012
Col1a1	1,891	11,943	20,881	11,581	16,530	19,236
Cspg4	21	81	232	16	141	294
Cygb	27	58	137	75	178	188
Des	33	175	306	315	392	562
Eln	22	316	1,773	970	944	1,014
Entpd2	12	22	12	66	42	61
Fbln2	25	265	1,995	152	1,612	586
Foxf1a	205	1,776	7,981	2,493	7,003	6,538
Gata4	139	1,582	5,354	993	5,522	7,689
Hlx	75	326	1,359	675	2,656	3,925
Jag1	268	963	1,587	1,042	1,313	2,277
Lhx2	21	111	262	427	595	1,313
Nes	35	222	486	176	617	1,147
Ngfr	36	84	154	436	602	2,466
Thy1	20	37	3	55	49	216

Symbol	Liver	ALCAM+	ALCAM+ PDPN+ MCs	ALCAM+ PDPN− cells	ALCAM+ ITGA8− MCs	ALCAM+ ITGA8+ cells
Vim	3,040	9,704	18,616	11,008	17,710	18,928

Table 2

Microarray analysis: Expression of integrins and cytokines/growth factors.

Symbol	Liver	ALCAM+	ALCAM+ PDPN+ MCs	ALCAM+ PDPN− cells	ALCAM+ ITGA8− MCs	ALCAM+ ITGA8+ cells
Integrins						
Itga1	281	400	1,577	2,163	1,206	1,294
Itga5	258	914	2,222	4,436	2,555	5,117
Itga8	48	430	737	2,215	871	4,354
Itga9	96	213	84	74	848	1,479
Itgav	845	4,218	14,600	13,358	12,458	13,343
Itgb1	1,084	1,683	2,542	2,274	2,380	1,733
Itgb3	1,348	5,611	5,403	238	3,244	6,252
Itgb5	99	396	1,357	2,213	1,033	2,279
Itgb8	6	89	202	29	886	723
Cytokines/Growth factors						
Fgf9	59	614	1,551	85	1,332	324
Fgf11	9	97	228	150	830	616
Fgf13	165	177	353	87	744	841
Fgf18	28	144	630	25	684	313
HGF	39	73	254	314	856	495
Mdk	359	3,214	9,292	3,971	8,620	9,642
Osm	48	25	101	4	33	61
Pdgfa	205	1,929	7,534	2,210	4,242	1,666
Pdgfb	36	30	35	30	60	43
Pdgfc	230	3,293	11,784	905	12,096	9,403
Pdgfd	104	306	2,943	243	1,067	459
Ptn	1,351	4,437	13,947	8,801	12,655	14,213
Tgfb1	214	492	207	92	889	1,552
Tgfb2	349	2,932	3,932	390	8,778	9,541
Tnf	28	28	64	61	24	33
Vegfa	111	432	1,890	2,594	2,308	2,781

Symbol	Liver	ALCAM+	ALCAM+ PDPN+ MCs	ALCAM+ PDPN− cells	ALCAM+ ITGA8− MCs	ALCAM+ ITGA8+ cells
Vegfb	106	256	623	929	593	1,060
Vegfc	43	373	1,273	1,969	2,143	4,324
Wnt4	36	128	454	108	618	865
Wnt5a	13	164	643	32	387	169
Wnt5b	18	515	1,694	131	1,128	1,452
Wnt9b	11	457	2,052	74	1,723	1,083
Wnt11	71	123	334	146	372	188